Contribution of Polar Groups in the Interior of a Protein to the Conformational Stability[†,‡]

Kazufumi Takano,[§] Yuriko Yamagata,[||] and Katsuhide Yutani*[,§]

Institute for Protein Research, Osaka University, Yamadaoka, Suita, Osaka 565-0871, Japan, and Graduate School of Pharmaceutical Sciences, Osaka University, Yamadaoka, Suita, Osaka 565-0871, Japan

Received December 8, 2000; Revised Manuscript Received February 5, 2001

ABSTRACT: It has been generally believed that polar residues are usually located on the surface of protein structures. However, there are many polar groups in the interior of the structures in reality. To evaluate the contribution of such buried polar groups to the conformational stability of a protein, nonpolar to polar mutations (L8T, A9S, A32S, I56T, I59T, I59S, A92S, V93T, A96S, V99T, and V100T) in the interior of a human lysozyme were examined. The thermodynamic parameters for denaturation were determined using a differential scanning calorimeter, and the crystal structures were analyzed by X-ray crystallography. If a polar group had a heavy energy cost to be buried, a mutant protein would be remarkably destabilized. However, the stability (ΔG) of the Ala to Ser and Val to Thr mutant human lysozymes was comparable to that of the wild-type protein, suggesting a low-energy penalty of buried polar groups. The structural analysis showed that all polar side chains introduced in the mutant proteins were able to find their hydrogen bond partners, which are ubiquitous in protein structures. The empirical structure-based calculation of stability change ($\Delta\Delta G$) [Takano et al. (1999) *Biochemistry 38*, 12698−12708] revealed that the mutant proteins decreased the hydrophobic effect contributing to the stability (ΔG_{HP}), but this destabilization was recovered by the hydrogen bonds newly introduced. The present study shows the favorable contribution of polar groups with hydrogen bonds in the interior of protein molecules to the conformational stability.

In folded proteins, the side chains of hydrophobic amino acid residues are generally buried in the interior of the proteins. A total of 81% of the nonpolar side chains are buried out of contact with water (*1*), and the hydrophobic interaction plays important roles in protein folding and stability (*2*). The contribution of such hydrophobic interactions to protein stability has been extensively investigated with mutant proteins (*3*−*13*). Pace (*14*) has shown that a buried methylene group contributes 5.4 kJ/mol (1.3 kcal/mol) on the average to the protein stability.

In contrast to the nonpolar residues, it has been postulated that polar residues are generally located on the surface of protein structures and that buried polar groups are unfavorable for the conformational stability. Some studies based on transfer experiments of amino acid residues (amino acid analogues or model compounds) from organic solvents or vacuum to water have shown that introducing a polar group in the interior of a protein should involve a significant energetic penalty (*15*, *16*). However, 63% of polar side chains and 70% of peptide groups are still buried inside the protein molecules (*1*), and the transfer Gibbs energies (ΔG_{trans}) for polar residues are highly dependent on the nonaqueous environments (*17*). Furthermore, the effects of such buried polar groups (buried polar surface) on protein stability have not yet been well examined with mutant proteins, even though mutational analysis is a useful approach for estimating the contribution of some factors to the conformational stability of a protein. The role of the buried polar groups in the stability thus remains controversial. Recently, our study using mutant protein experiments has suggested that the dehydration of polar groups hardly affects protein stability (*18*).

In the present study, we examined 11 mutant human lysozymes, L8T, A9S, A32S, I56T, I59T, I59S, A92S, V93T, A96S, V99T, and V100T, in which a buried nonpolar residue was substituted with a polar one, to estimate the contribution of polar groups in the interior of the molecule to the conformational stability. Figure 1 shows the structure of a human lysozyme and the mutation residues. These residues are completely buried in the molecules. The DSC measurements of the mutant proteins were carried out, and the crystal structures were determined. The results confirm the proposition of our previous study (*18*) that buried polar groups with hydrogen bonds favorably contribute to the stability.

MATERIALS AND METHODS

Mutant Proteins. Mutagenesis, expression, and purification of mutant human lysozymes examined in this study were

[†] This work was supported in part by Fellowships from the Japan Society for the Promotion of Science for Young Scientists (K.T.), by a Grant-in-Aid for Scientific Research on Priority Areas (C) "Genome Information Science" from the Ministry of Education, Science, Sports and Culture of Japan (K.Y.), and by the Structural Biology Sakabe Project (K.Y. and Y.Y.).

[‡] The coordinates have been deposited in the Protein Data Bank under PDB filenames L8T, 1GEV; A9S, 1GEZ; A32S, 1GF0; A92S, 1GF3; V93T, 1GF4; A96S, 1GF5; V99T, 1GF6; V100T, 1GF7.

* To whom correspondence should be addressed. Phone: +81-6-6879-8615. Fax: +81-6-6879-8616. E-mail: yutani@protein.osaka-u.ac.jp.

[§] Institute for Protein Research, Osaka University.

[||] Graduate School of Pharmaceutical Sciences, Osaka University.

[1] Abbreviations: ASA, accessible surface area; DSC, differential scanning calorimetry; T_d, denaturation temperature.

10.1021/bi002792f CCC: $20.00
Published on Web 03/21/2001

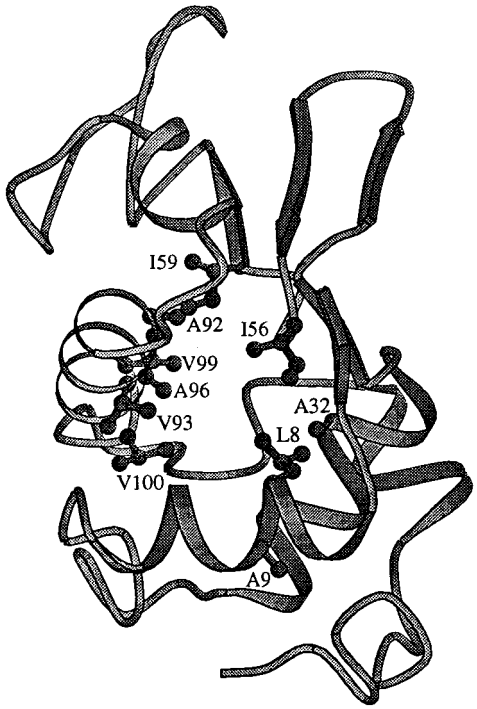

FIGURE 1: Structure of human lysozyme (*11*). The residues modified in this study are shown. The structure was generated with the program MOLSCRIPT (*49*).

performed as described (*11*). All chemicals were reagent grade. Protein concentration of the mutant proteins was determined spectrophotometrically using $E^{1\%}(1\text{ cm}) = 25.65$ at 280 nm (*19*).

Differential Scanning Calorimetry (DSC). Calorimetric measurements were carried out with a DASM4 microcalorimeter. The buffer solution used was 0.05 M Gly-HCl. Each protein was measured three or four times at different pH points between pH 2.4 and 3.4. The data analysis of DSC was done using the Origin software (MicroCal, Inc., MA), as described previously (*11*). The thermodynamic parameters for denaturation as a function of temperature were calculated using the following equations (*20*),

$$\Delta H(T) = \Delta H(T_d) - \Delta C_p(T_d - T) \quad (1)$$

$$\Delta S(T) = \Delta H(T_d)/T_d - \Delta C_p \ln(T_d/T) \quad (2)$$

$$\Delta G(T) = \Delta H(T) - T\Delta S(T) \quad (3)$$

assuming that ΔC_p does not depend on temperature.

X-ray Crystal Analysis. The mutant human lysozymes examined in this study were crystallized at pH 4.5 as described previously (*11*, *21*). All of the crystals belong to the space group $P2_12_12_1$ with a crystal form identical to that of the wild-type protein (*11*). The crystal structures of I56T, I59T, and I59S have already been determined (*18*, *22*).

Intensity data sets of the mutant human lysozymes were collected with a Weissenberg camera (*23*) on beam line 18B at the Photon Factory (Tsukuba, Japan; proposal no. 99G099) for A32S, and with a Rigaku R-AXIS IV imaging plate (Tokyo, Japan) at the Institute for Protein Research, Osaka University (Suita, Japan) for L8T, A9S, A92S, V93T, A96S, V99T, and V100T. The data were processed with the program DENZO (*24*). The structures were solved by the isomorphous method and refined with the program X-PLOR (*25*) as described previously (*11*, *21*).

Table 1: Thermodynamic Parameters for Denaturation of Mutant Human Lysozymes at 64.9 °C, pH 2.7

	T_d (°C)	ΔT_d (°C)	ΔC_p (kJ/mol K)	ΔH (kJ/mol)	$\Delta\Delta H^a$ (kJ/mol)	$\Delta\Delta G^b$ (kJ/mol)
wild-type[c]	64.9		6.6	477		
L8T	52.5	−12.4	5.8	446	−31	−15.6
A9S	64.8	−0.1	5.3	444	−33	−0.1
A32S	63.9	−1.0	6.9	463	−14	−1.4
I56T[d]	52.4	−12.5	4.5	425	−52	−15.2
I59S[e]	53.1	−11.8	5.6	447	−30	−15.0
I59T[e]	58.0	−6.9	6.4	470	−7	−9.3
A92S	67.5	+2.6	8.4	434	−43	+3.4
V93T	62.6	−2.3	4.7	421	−56	−2.8
A96S	61.6	−3.3	5.4	432	−45	−4.2
V99T	63.3	−1.6	5.9	437	−40	−2.1
V100T	64.0	−0.9	6.4	447	−30	−1.2

[a] $\Delta\Delta H = \Delta H$ (mutant) − ΔH (wild). [b] $\Delta\Delta G = \Delta G$ (mutant) − ΔG (wild). [c] Takano et al. (*11*). [d] Funahashi et al. (*22*). [e] Funahashi et al. (*18*).

RESULTS

DSC Measurements of the Mutant Human Lysozymes. To measure the changes in conformational stability of the mutant human lysozymes, we examined the heat denaturation of the mutant proteins by DSC. The DSC measurements were carried out in the acidic pH region (pH 2.4−3.4) where the heat denaturation of human lysozyme is highly reversible. Table 1 shows the thermodynamic parameters for denaturation of the mutant and wild-type proteins at the same temperature, 64.9 °C, which is the denaturation temperature of the wild-type at pH 2.7 (*11*).

The stability changes ($\Delta\Delta G$) of buried Val to Thr mutant proteins ranged from −1.2 to −2.8 kJ/mol (Table 1). These values are quite different from the difference in ΔG_{trans} between Val and Thr (about −30 kJ/mol) calculated using the ΔG_{trans} of cyclohexane or vacuum (*26*, *27*). The result suggests that the buried polar residues do not greatly contribute to the destabilization of protein. The stability changes in Ala to Ser mutant proteins were also small (less than 5 kJ/mol), but the mutations of Leu/Ile to Thr/Ser greatly decreased the stability (more than 9 kJ/mol). These stability changes ($\Delta\Delta G$) could be explained by the empirical calculation based on structural changes due to mutations (*18*, *28*) (see Discussion).

Crystal Structures of the Mutant Human Lysozymes. To investigate the structural changes due to mutation, we determined the crystal structures of the mutant human lysozymes by X-ray analysis. Data collection and refinement statistics of the mutant proteins are summarized in Table 2. The overall structures of the mutant proteins examined are similar to that of the wild-type protein. The superimposed structures of the wild-type and each mutant protein in the vicinity of mutation site are illustrated in Figure 2. Every polar side chain introduced in the interior of the molecule forms new hydrogen bonds with polar groups around the site. This indicates that polar groups in the interior of a protein are prone to form hydrogen bonds. In the structures of I59S, I59T (*18*), and V93T, new water molecules are observed near the mutation site and form hydrogen bonds with the mutation residue.

Table 2: X-ray Data Collection and Refinement Statistics of Mutant Human Lysozymes

	L8T	A9S	A32S	A92S	V93T	A96S	V99T	V100T
				(A) Data Collection				
cell (Å)								
a	56.42	56.24	56.36	56.18	56.17	56.32	56.42	56.34
b	60.68	61.23	61.56	61.32	61.25	61.22	61.28	61.45
c	32.90	32.88	32.70	32.76	32.76	32.85	32.59	32.69
resolution	2.1	1.8	1.8	1.8	1.8	1.8	1.8	1.8
no. of measured reflections	17 508	34 540	48 127	34 266	34 979	34 963	24 628	34 569
no. of independent reflections	5442	10 750	10 999	10 831	10 846	10 946	10 383	10 871
completeness (%)	76.3	97.1	99.9	98.2	98.4	98.8	94.2	98.2
R_{merge} (%)[a]	7.0	4.3	4.0	3.4	4.1	4.3	3.6	4.3
				(B) Refinement				
no. of protein atoms	1028	1030	1030	1030	1029	1030	1029	1029
no. of solvent atoms	193	270	247	251	263	260	239	252
resolution (Å)	8.0−2.1	8.0−1.8	8.0−1.8	8.0−1.8	8.0−1.8	8.0−1.8	8.0−1.8	8.0−1.8
no. of used reflections	4957	9476	10 526	10 190	8818	8620	9156	9939
completeness (%)	72.4	87.1	96.6	94.0	81.4	79.2	84.6	91.4
R-factor[b]	0.156	0.167	0.172	0.172	0.173	0.172	0.170	0.170

[a] $R_{merge} = 100 \times \sum|I - \langle I\rangle|/\sum\langle I\rangle$. [b] $R\text{-factor} = \sum||F_o| - |F_c||/\sum|F_o|$.

Some systematic surveys of hydrogen bonds in protein structures have shown that buried polar groups usually find their hydrogen bond partners and are rarely left unsatisfied (*29*−*32*). This is because more than half of all polar groups are buried within the molecular interior, and hydrogen bonding partners are omnipresent within protein structures (*1*, *33*, *34*). In the case of the buried polar side chains examined in this study, there are at least some polar groups around them, such as the neighbor backbone nitrogen/oxygen atoms and their hydrogen bond partners. The Ser/Thr side chain introduced in A9S, V93T, and V100T mutant human lysozymes forms a hydrogen bond with its neighbor backbone atom, and that in L8T, A32S, I56T, A96S, and V99T forms a hydrogen bond with its backbone hydrogen bond partner (Figure 2).

DISCUSSION

Empirical Structure-Based Calculation of Stability Change (ΔΔG) Using the Wild-Type and Mutant Structures. Amino acid substitutions affect the conformational stability by a combination of the contributions of several stabilization factors, such as hydrophobic effects, hydrogen bonds, and entropic effects. In the present case, all mutant proteins examined would affect hydrophobic interaction (*12*, *13*), side-chain conformational entropy of mutation residues in the denatured state (*35*), and hydrogen bonds (*21*, *28*, *36*). Furthermore, the crystal structures of I59S, I59T (*18*), and V93T revealed that new water molecules appear at the mutation site (Figure 2). Because a water molecule affects protein stability (*28*, *37*, *38*), the stability changes in I59S, I59T, and V93T should include the effect of such water molecules.

It has been proposed that the stability change in each mutant protein is represented by a unique equation, considering the conformational changes due to mutations (*18*, *28*).

$$\Delta\Delta G_{est} = \Delta\Delta G_{HP} + \Delta\Delta G_{ent} + \Delta\Delta G_{HB} + \Delta\Delta G_{H_2O} + \Delta\Delta G_{other} \quad (4)$$

where $\Delta\Delta G_{HP}$, $\Delta\Delta G_{ent}$, $\Delta\Delta G_{HB}$, $\Delta\Delta G_{H_2O}$, and $\Delta\Delta G_{other}$ represent the changes in ΔG due to a hydrophobic effect, the side chain conformational entropy of the mutation residue, forming and removing hydrogen bonds, introducing water molecules, and the contribution of other effects to stability, respectively. Each $\Delta\Delta G$ can be expressed by each parameter in terms of the conformational change as shown in the following equations.

$$\Delta\Delta G_{HP} = 0.178\Delta\Delta ASA_{NP} - 0.013\Delta\Delta ASA_{P} \quad (5)$$

$$\Delta\Delta G_{ent} = -T\Delta\Delta S_{conf} \quad (6)$$

$$\Delta\Delta G_{HB} = 25.63\sum(r_{HB[pp]})^{-1} + 15.60\sum(r_{HB[pw]})^{-1} + 14.91\sum(r_{HB[ww]})^{-1} \quad (7)$$

$$\Delta\Delta G_{H_2O} = -7.79\,\Delta N_{H_2O} \quad (8)$$

where ΔASA_{NP} and ΔASA_{P} represent the differences in ASA (accessible surface area) of the nonpolar (C/S) and polar (O/N) atoms, respectively, of all residues in a protein upon denaturation, and ΔΔASA means the difference in ΔASA between the wild-type and mutant proteins (*12*, *18*); ΔS_{conf} is the difference in the side chain conformational entropy defined by Doig and Sternberg (*35*); $r_{HB[pp]}$, $r_{HB[pw]}$, and $r_{HB[ww]}$ are the length of the hydrogen bond between protein atoms, between a protein atom and a water molecule, and between water molecules, respectively (*28*); N_{H_2O} is the number of water molecules introduced by substitution (*28*).

As previously discussed by Funahashi et al. (*18*), eq 5 means that buried nonpolar groups (buried nonpolar surface) greatly contribute to the protein stability (the coefficient of $\Delta\Delta ASA_{NP}$, 0.178, in eq 5), whereas the dehydration of polar groups has little effect on the stability (the coefficient of $\Delta\Delta ASA_{P}$, −0.013, in eq 5). These coefficients (0.178 and −0.013) are comparable to the values estimated from the transfer Gibbs energy from water to octanol, 0.13 and −0.004, respectively (*39*), rather than those from water to vacuum, 0.05 and −0.5, respectively (*15*). Equation 7, furthermore, respects the contributions of hydrogen bonds to protein stability. These parameters could be useful for the analysis of the present data from the buried nonpolar to polar mutant proteins.

Figure 3 shows the correlation between $\Delta\Delta G_{exp}$ and $\Delta\Delta G_{est}$ using eq 4 ($\Delta\Delta G_{other} = 0$) for the 11 mutant human

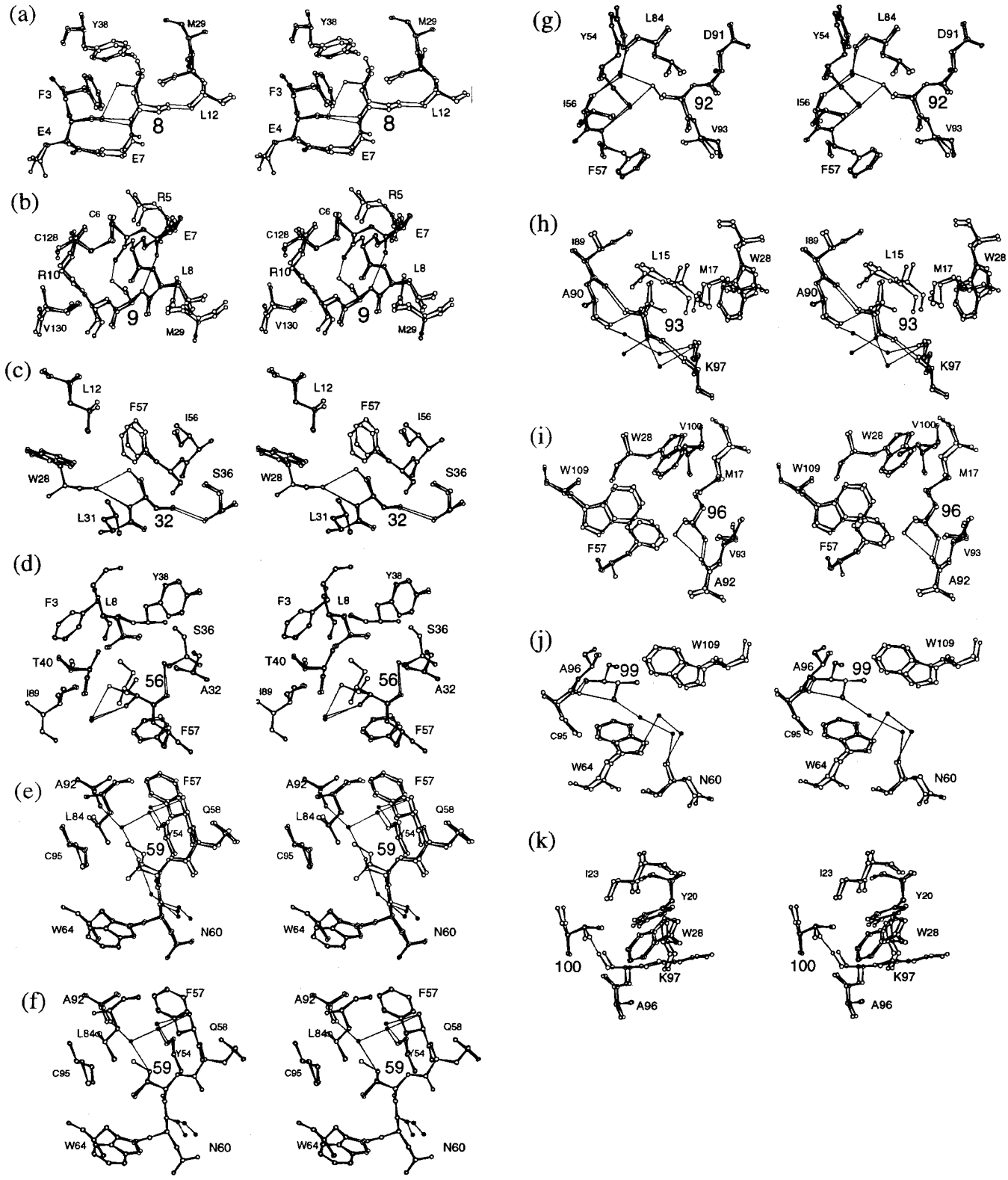

FIGURE 2: Stereodrawings of the structures in the vicinity of the mutation sites for (a) L8T, (b) A9S, (c) A32S, (d) I56T (*22*), (e) I59S (*18*), (f) I59T (*18*), (g) A92S, (h) V93T, (i) A96S, (j) V99T, and (k) V100T human lysozymes. The wild-type and mutant structures are superimposed. The thin lines and filled circles represent hydrogen bonds and water molecules, respectively.

lysozymes examined in this paper. The estimated stability roughly agrees with the experimental stability, except for L8T. The stability of L8T is about 6 kJ/mol lower than the estimated value. This suggests that the difference between them contains the contribution of other factors to stability, which are not considered in the present calculation. The structural analysis of L8T showed that the Oγ atom of Thr8 in the mutant structure has a short contact with the Cβ atom of Phe3 (2.99 Å), resulting from the steric difference in shape between Leu and Thr residues. Because unfavorable steric interactions severely destabilized protein structures (*3*, *18*, *40*), the difference in L8T between $\Delta\Delta G_{exp}$ and $\Delta\Delta G_{est}$ might

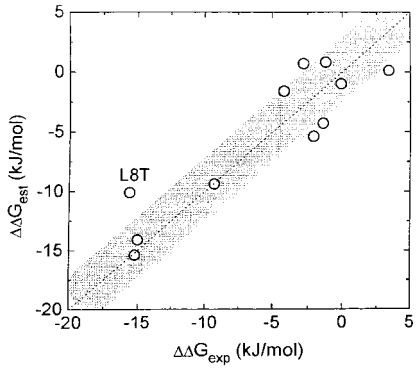

FIGURE 3: Relation between the experimental $\Delta\Delta G$ value ($\Delta\Delta G_{exp}$) and estimated $\Delta\Delta G$ value ($\Delta\Delta G_{est}$) for the mutant human lysozymes. The $\Delta\Delta G_{exp}$ value is from Table 1, and the $\Delta\Delta G_{est}$ value is calculated using eq 4. The gray region represents the standard deviation of the data (SD = 3.1).

Table 3: Contribution of Various Factors to the Stability of Mutant Human Lysozymes (kJ/mol)

	$\Delta\Delta G_{exp}$[a]	$\Delta\Delta G_{est}$[b]	$\Delta\Delta G_{HP}$[c]	$\Delta\Delta G_{HB}$[d]	$\Delta\Delta G_{H_2O}$[e]	$\Delta\Delta G_{ent}$[f]
L8T	−15.6	−10.1	−16.7	+8.3		−1.7
A9S	−0.1	−1.0	−4.6	+8.8		−5.2
A32S	−1.4	−4.3	−8.1	+9.0		−5.2
I56T	−15.2[g]	−15.4	−19.0	+5.1		−1.5
I59S	−15.0[g]	−13.6	−23.4	+26.6	−15.1	−1.7
I59T	−9.3[g]	−9.1	−16.8	+16.7	−7.5	−1.5
A92S	+3.4	+0.1	−5.4	+10.7	-	−5.2
V93T	−2.8	+0.7	−4.6	+15.9	−7.5	−3.1
A96S	−4.2	−1.6	−5.7	+9.3		−5.2
V99T	−2.1	−5.4	−11.0	+8.7		−3.1
V100T	−1.2	+0.8	−5.0	+8.9		−3.1

[a] The experimental $\Delta\Delta G$ values (Table 1). [b] The $\Delta\Delta G$ values were estimated using eq 4 ($\Delta\Delta G_{est} = \Delta\Delta G_{HP} + \Delta\Delta G_{HB} + \Delta\Delta G_{H_2O} + \Delta\Delta G_{ent}$). [c] The $\Delta\Delta G_{HP}$ values were estimated using eq 5. [d] The $\Delta\Delta G_{HB}$ values were estimated using eq 7. [e] The $\Delta\Delta G_{H_2O}$ values were estimated using eq 8. [f] The $\Delta\Delta G_{ent}$ values were estimated using eq 6. [g] Funahashi et al. (*18*).

be compensated if the effect of the local steric strain can be considered. Table 3 lists the contribution of each factor to the mutant stability estimated from eq 4. All mutant proteins decrease the ΔG_{HP} values due to the buried nonpolar to polar mutations. This destabilization, however, is compensated by the formation of the hydrogen bonds in most mutant proteins. This result confirms the favorable contribution of buried polar groups with hydrogen bonds to protein stability.

Contribution of Buried Polar Side Chains to Protein Stability. The transfer Gibbs energy, ΔG_{trans}, of amino acid residues from organic solvents or vacuum to water as a hydrophobicity scale has been used to estimate the contribution of buried residues to the stability of proteins (*41*). To date, various hydrophobicity scales have been proposed based on transfer experiments using different organic solvents or vapor phase (*26*, *27*, *42*−*46*). Table 4 summarizes three ΔG_{trans} values of side chains for Ile, Leu, Val, Ala, Thr and Ser residues. There are large differences among such scales depending on the nonaqueous phase.

Here, we can offer a new scale for the contribution of buried amino acid side chains to protein stability (ΔG_{SC}) based on the empirical calculation of stability change as shown in eq 4, which is obtained from the real experimental data upon protein denaturation. The ΔG_{SC} values for Ile, Leu, Val, Ala, Thr, and Ser residues are also shown in Table 4. The ΔG_{SC} value includes the hydrophobic effect (ΔG_{HP}), side chain entropy change (ΔG_{ent}) and effects of hydrogen bonds (ΔG_{HB}). The ΔG_{HP} value may correspond to the ΔG_{trans} values.

The buried polar residues, Ser and Thr, have a relatively smaller contribution from a hydrophobic effect (ΔG_{HP}) than buried nonpolar residues. However, the ΔG_{HP} values of the polar residues are positive, indicating that the polar residues also contribute to protein stability through the hydrophobic effect. Furthermore, the buried polar residues, Ser and Thr, additionally contribute to the stability, if the buried polar residues form one or two intramolecular hydrogen bonds. In fact, most polar groups find their hydrogen bond partners in the interior of a protein, and the side chains of Ser and Thr form 2.3 hydrogen bonds on the average (*32*). Recently, Pace (*47*) has pointed out in another way a greater contribution of buried polar groups to protein stability than that of buried nonpolar groups.

CONCLUSIONS

There are many studies on hydrophobic mutants of proteins, indicating that hydrophobic residues in the interior contribute to the conformational stability. In contrast, the role of buried polar groups in the stability was still unclear, although they are ubiquitous in the molecular interior. In the present study, the stability and structure of 11 mutant human lysozymes in which a buried nonpolar residue is replaced by a polar one have been examined. The results show that buried polar groups are not a destabilization factor in protein structure but play an important role in the protein stabilization through the formation of hydrogen bonds. This

Table 4: Three ΔG_{trans} Values of Side Chains for Amino Acid Residues and Contribution of Buried Side Chains for Amino Acid Residues to Protein Stability (kJ/mol)

	ΔG_{trans}[a]			ΔG_{SC}[e]				ΔG_{HB}[g]			
	vapor[b]	chex[c]	oct[d]	0_{HB}[i]	1_{HB}[i]	2_{HB}[i]	ΔG_{HP}[f]	0_{HB}[i]	1_{HB}[i]	2_{HB}[i]	ΔG_{ent}[h]
Leu	−0.5	16.7	9.7	21.0			24.4				−3.4
Ile	−1.0	16.7	10.3	21.3			24.9				−3.6
Val	−1.7	12.9	6.9	18.8			20.8				−2.0
Ala	−1.9	3.6	1.8	11.9			11.9				0
Ser	−31.2	−18.2	−0.2	2.2	10.7	19.2	7.4	0	8.5	17.0	−5.2
Thr	−30.4	−14.7	1.5	7.7	16.2	24.7	12.8	0	8.5	17.0	−5.1

[a] ΔG_{trans} values between each amino acid and Gly residues. [b] The ΔG_{trans} values for vapor to water (*26*). [c] The ΔG_{trans} values for cyclohexane (Chex) to water (*27*). [d] The ΔG_{trans} values for octanol (Oct) to water (*44*). [e] $\Delta G_{SC} = \Delta G_{HP} + \Delta G_{HB} + \Delta G_{ent}$. [f] $\Delta G_{HP} = 0.178\ ASA_{NP} - 0.013\ ASA_P$, where ASA_{NP} and ASA_P are the ASA values of nonpolar and polar atoms, respectively, for each amino acid side chain (*48*). [g] ΔG_{HB} is a hydrogen bond contribution when an amino acid residue has no, one, or two intramolecular hydrogen bonds with 3 Å length (*28*). [h] ΔG_{ent} is the change in side chain conformational entropy upon denaturation (*35*). [i] The number of intramolecular hydrogen bonds.

means that protein structures are stabilized not only by buried nonpolar groups but also by buried polar groups with hydrogen bonds. We also showed a new scale for the contribution of buried amino acid side chains to protein stability (ΔG_{SC}).

ACKNOWLEDGMENT

We thank Takeda Chemical Ind., Ltd. (Osaka, Japan), for providing plasmid pGEL125.

REFERENCES

1. Lesser, G. J., and Rose, G. D. (1990) *Proteins: Struct., Funct., Genet. 8*, 6−13.
2. Dill, K. A. (1990) *Biochemistry 29*, 7133−7155.
3. Yutani, K., Ogasahara, K., Tsujita, T., and Sugino, Y. (1987) *Proc. Natl. Acad. Sci. U.S.A. 84*, 4441−4444.
4. Matsumura, M., Becktel, W., and Matthews, B. W. (1988) *Nature 334*, 406−410.
5. Kellis, J. T., Jr., Nyberg, K., Sali, D., and Fersht, A. R. (1988) *Nature 333*, 784−786.
6. Shortle, D., Stites, W. E., and Meeker, A. K. (1990) *Biochemistry 29*, 8033−8041.
7. Sandberg, W. S., and Terwilliger, T. C. (1991) *Proc. Natl. Acad. Sci. U.S.A. 88*, 1706−1710.
8. Lim, W. A., and Sauer, R. T. (1991) *J. Mol. Biol. 219*, 359−376.
9. Eriksson, A. E., Baase, W. A., Zhang, X.-J., Heinz, D. W., Blaber, M., Baldwin, E. P., and Matthews, B. W. (1992) *Science 255*, 178−183.
10. Ishikawa, K., Nakamura, H., Morikawa, K., and Kanaya, S. (1993) *Biochemistry 32*, 6171−6178.
11. Takano, K., Ogasahara, K., Kaneda, H., Yamagata, Y., Fujii, S., Kanaya, E., Kikuchi, M., Oobatake, M., and Yutani, K. (1995) *J. Mol. Biol. 254*, 62−76.
12. Takano, K. Yamagata, Y., Fujii, S., and Yutani, K. (1997) *Biochemistry 36*, 688−698.
13. Takano, K., Yamagata, Y., and Yutani, K. (1998) *J. Mol. Biol. 280*, 749−761.
14. Pace, C. N. (1992) *J. Mol. Biol. 226*, 29−35.
15. Wesson, L., and Eisenberg, D. (1992) *Protein Sci. 1*, 227−235.
16. Honig, B., and Cohen, F. E. (1996) *Folding Des. 1*, R17−20.
17. Karplus, P. A. (1997) *Protein Sci. 6*, 1302−1307.
18. Funahashi, J., Takano, K., Yamagata, Y., and Yutani, K. (1999) *Protein Eng. 12*, 841−850.
19. Parry, R. M., Chandan, R. C., and Shahani, K. M. (1969) *Arch. Biochem. Biophys. 130*, 59−65.
20. Privalov, P. L., and Khechinashvili, N. N. (1974) *J. Mol. Biol. 86*, 665−684.
21. Yamagata, Y., Kubota, M., Sumikawa, Y., Funahashi, J., Takano, K., Fujii, S., and Yutani, K. (1998) *Biochemistry 37*, 9355−9362.
22. Funahashi, J., Takano, K., Ogasahara, K., Yamagata, Y., and Yutani, K. (1996) *J. Biochem. 120*, 1216−1223.
23. Sakabe, N. (1991) *Nucl. Instr. Methods Phys. Res. A 303*, 448−463.
24. Otwinowski, Z. (1990) *DENZO data processing package*, Yale University, New Haven, CT.
25. Brunger, A. T. (1992) X-*PLOR Manual*, Ver. 3.1, Yale University, New Haven, CT.
26. Wolfenden, R., Andersson, L., Cullis, P. M., and Southgate, C. C. B. (1981) *Biochemistry 20*, 849−855.
27. Radzika, A., and Wolfenden, R. (1988) *Biochemistry 27*, 1644−1670.
28. Takano, K., Yamagata, Y., Funahashi, J., Hioki, Y., Kuramitsu, S., and Yutani, K. (1999) *Biochemistry 38*, 12698−12708.
29. Baker, E. N., and Hubbard, R. E. (1984) *Prog. Biophys. Mol. Biol. 44*, 97−179.
30. Ippolito, J. A., Alexander, R. S., and Christianson, D. W. (1990) *J. Mol. Biol. 215*, 457−471.
31. Stickle, D. F., Presta, L. G., Dill, K. A., and Rose, G. D. (1992) *J. Mol. Biol. 226*, 1143−1159.
32. McDonald, I. K., and Thornton, J. M. (1994) *J. Mol. Biol. 238*, 777−793.
33. Chothia, C. (1976) *J. Mol. Biol. 105*, 1−14.
34. Richards, F. M. (1977) *Annu. Rev. Biophys. Bioeng. 6*, 151−176.
35. Doig, A. J., and Sternberg, M. J. E. (1995) *Protein Sci. 4*, 2247−2251.
36. Takano, K., Yamagata, Y., Kubota, M., Funahashi, J., Fujii, S., and Yutani, K. (1999) *Biochemistry 38*, 6623−6629.
37. Takano, K., Funahashi, J., Yamagata, Y., Fujii, S., and Yutani, K. (1997) *J. Mol. Biol. 274*, 132−142.
38. Takano, K., Tsuchimori, K., Yamagata, Y., and Yutani, K. (1999) *Eur. J. Biochem. 266*, 675−682.
39. Vajda, S., Weng, Z., Rosenfeld, R., and DeLisi, C. (1994) *Biochemistry 33*, 13977−13988.
40. Liu, R., Baase, W. A., and Matthews, B. W. (2000) *J. Mol. Biol. 295*, 127−145.
41. Tanford, C. (1962) *J. Am. Chem. Soc. 84*, 4240−4247.
42. Nozaki, Y., and Tanford, C. (1971) *J. Biol. Chem. 246*, 2211−2217.
43. Fendler, J., Nome, F., and Nagyvary, J. (1975) *J. Mol. Evol. 6*, 215−232.
44. Fauchere, J.-L., and Pliska, V. (1974) *Eur. J. Med. Chem. 18*, 369−375.
45. Damodaran, S., and Song, K. B. (1986) *J. Biol. Chem. 261*, 7220−7222.
46. Privalov, P. L., and Makhatadze, G. I. (1993) *J. Mol. Biol. 232*, 660−679.
47. Pace, C. N. (2001) *Biochemistry 40*, 310−313.
48. Miller, S., Janin, J., Lesk, A. M., and Chothia, C. (1987) *J. Mol. Biol. 196*, 641−656.
49. Kraulis, P. J. (1991) *J. Appl. Crystallogr. 24*, 946−950.

BI002792F